Alternating Site Mechanism of the Kinesin ATPase[†]

Susan P. Gilbert,[‡] Michele L. Moyer, and Kenneth A. Johnson*

Department of Biochemistry and Molecular Biology, 106 Althouse Laboratory, Pennsylvania State University, University Park, Pennsylvania 16802

Received May 13, 1997; Revised Manuscript Received September 26, 1997

ABSTRACT: The processivity of the microtubule−kinesin ATPase has been investigated using stopped-flow kinetic methods to measure the binding of each motor domain of the dimeric kinesin (K401) to the microtubule and the release of the fluorescent ADP analog, 2′(3′)-*O*-(*N*-methylanthraniloyl)adenosine 5′-diphosphate (mantADP) from the active site of the motor domain. The results show that the release of two molecules of ADP from dimeric kinesin (K401) after the binding of kinesin·ADP to the microtubule is a sequential process leading to biphasic kinetics. The maximum rate of release of mantADP from the first motor domain of K401 or monomeric K341 is fast (300 s^{-1}) and independent of added nucleotide. The rate of mantADP release from the second motor domain of K401 is slow in the absence of added nucleotide (0.4 s^{-1}) and reaches a maximum rate of 300 s^{-1} at saturating concentrations of ATP. High concentrations of ADP stimulate mantADP release from the second head to a maximum rate of 3.8 s^{-1}. The nonhydrolyzable analog AMP-PNP and ATP-γS also stimulate ADP release from the second head (maximum rate of 30 s^{-1}), suggesting that ATP hydrolysis is not necessary to stimulate the ADP release. These experiments establish an alternating site mechanism for dimeric kinesin whereby ATP binding to one kinesin active site stimulates the release of ADP from the second site such that the reactions occurring at the active sites of the two monomer units are kept out of phase from each other by interactions between the heads. These results define the steps of the ATPase pathway that lead to the efficient coupling of ATP hydrolysis to force production in a processive reaction whereby force production in forming a tight microtubule complex by one head is coupled to the rate-limiting release of the other head from the microtubule.

Kinesin is a cytoplasmic ATPase that drives the translocation of membranous organelles along microtubules toward the synapse in neurons. Kinesin as a single molecule, consisting of two motor domains, will promote translocation along a microtubule for several micrometers and at maximal velocities (Howard et al., 1989; Block et al., 1990). Thus, unlike skeletal muscle myosin or axonemal dynein, kinesin is presumed to hydrolyze multiple ATP molecules prior to detaching from the microtubule. Accordingly, kinesin has been designated a processive enzyme, and the degree of processivity has been defined in two ways. In motility assays where movement is analyzed, processivity is defined as the length of the translocation prior to the motor falling off the microtubule. In ATPase assays the processivity may be defined by the number of ATP molecules hydrolyzed per active site as the steady-state distribution of kinesin on and off the microtubule is approached. The processivity observed by motility can be correlated to ATP turnover because kinesin hydrolyses one ATP per 8-nm step (Hua et al., 1997; Schnitzer & Block, 1997).

Detailed studies using diverse approaches have been pursued to understand the mechanistic basis of processivity (Howard et al., 1989; Block et al., 1990; Correia et al., 1995; Moyer et al., 1996; Sadhu & Taylor, 1992; Romberg & Vale, 1993; Harrison et al., 1993; Song & Mandelkow, 1993; Ray et al., 1993; Svoboda et al., 1994; Huang et al., 1994; Gilbert & Johnson, 1994; Hunt et al., 1994; Gilbert et al., 1995; Berliner et al., 1995; Meyhöfer & Howard, 1995; Lockhart et al., 1995; Walker, 1995; Hirose et al., 1995; Lockhart et al., 1995; Ma & Taylor, 1995a;1995b; Hackney, 1995; Kull et al., 1996; Rosenfeld et al., 1996; Ma & Taylor, 1997a;1997b; Jiang & Hackney, 1997; Higuchi et al., 1997; Inoue et al., 1997; Schnitzer & Block, 1997; Hua et al., 1997). These studies have led to a model in which kinesin moves along the microtubule by a mechanism in which each motor domain of the dimer alternately interacts with the microtubule lattice (Hackney, 1994). Our kinetic experiments reported previously implied that the processivity was due in part to a sequential release of the two kinesin motor domains from the microtubule and a sequential rebinding of the motor domains to the microtubule (Gilbert et al., 1995). The experiments presented here measured the binding step directly, and the kinetic results with dimeric K401 and monomeric K341 (Correia et al., 1995; Moyer et al., 1996) show that binding of kinesin·ADP to the microtubule is also

[†] This work was supported by grants to K.A.J. (GM 26726 from the National Institutes of Health), to S.P.G. (Basil O'Connor Starter Scholar Research Award from the March of Dimes Birth Defects Foundation), and to M.L.M. (training grant GM 08358 from the National Institutes of Health).

* Author to whom correspondence should be addressed. Tel: (814) 865-1200. Fax : (814) 865-3030. E-mail: Kaj1@psu.edu.

[‡] Present address: 518 Langley Hall, Department of Biological Sciences, University of Pittsburgh, Pittsburgh, PA 15260. Tel: (412) 624-5842. E-mail: spg1+@pitt.edu.

S0006-2960(97)01117-3 CCC: $15.00
Published on Web 01/06/1998

a sequential process leading to biphasic ADP release. Furthermore, we present direct evidence for alternating site cooperativity whereby ATP binding to one kinesin site stimulates the release of ADP from the second site. These results reveal an important step in the ATPase pathway that leads to coordination of the interactions of the kinesin two heads with the microtubule lattice for processive movement. In the companion paper (Moyer et al., 1998), the kinetic mechanism of monomeric kinesin K341 is presented, and the kinetics of the individual steps of ATP binding, ATP hydrolysis, kinesin dissociation from the microtubule, and ADP and Pi release are compared to those for dimeric K401 to define the steps in the ATPase cycle that are controlled by the interaction between the motor domains.

EXPERIMENTAL PROCEDURES

Materials. Silica gel 60 F_{254} thin layer chromatography plates (EM Separations of E. Merck, 20 × 20 cm, plastic backed) were purchased from VWR Scientific (West Chester, PA), DEAE Sepharose FF from Pharmacia Biotech Inc. (Uppsala, Sweden), *N*-methylisatoic anhydride from Molecular Probes (Eugene, OR), and nucleotides from Pharmacia Biotech Inc. (ATP, 2′dATP) and Sigma Chemical Co. (3′dATP, AMP-PNP,[1] ATP-γ-S, St. Louis, MO).

Protein Purification. Bacterially expressed *Drosophila* K401 and K341 as well as bovine brain tubulin were purified as described previously (Gilbert & Johnson, 1993; Correia et al., 1995; Moyer et al., 1996). Microtubules were assembled from soluble tubulin (cold depolymerized and clarified) and stabilized with 20 μM taxol. Concentrations of K401 and K341 are expressed as the active site concentration on the basis of the binding of radiolabeled ADP (Gilbert & Johnson, 1993). In all experiments reported here, K401 is dimeric (K_d for dimerization at 37 nM) and K341 is monomeric to concentrations of at least 10 μM (Correia et al., 1995). All concentrations reported are final concentrations after mixing.

N-Methylanthraniloyl Nucleotide Analogs. Preparation of 2′(3′)-*O*-(*N*-methylanthraniloyl)adenosine 5′-triphosphate (mantATP), the mixture of 2′ and 3′- isomers of mantATP (or mantADP) were synthesized as described previously (Hiratsuka, 1983). The purity was confirmed by thin-layer chromatography (silica gel 60, F_{254} in 1-propanol/NH_4OH/water 6:3:1, v/v, containing 0.5 g L^{-1} EDTA), and the mantATP and mantADP showed the same absorption and fluorescence spectra as described previously (Hiratsuka, 1983). The A_{256}/A_{356} ratio for the mixture was 4 rather than 2.7, indicating that the fluorescent derivative was monosubstituted on either the 2′-position or the 3′-position rather than attachment to both 2′- and 3′-hydroxyl groups to form bismant derivatives (Moore & Lohman, 1994). 2′-mant-3′dATP and 3′-mant-2′dATP were also synthesized using 3′dATP and 2′dATP, respectively.

Stopped-Flow Experiments. A kinesin−mantADP complex (K·mantADP) was prepared by incubating 20 μM K401 or K341 (as purified with ADP tightly bound at the active site) with 40 μM mantADP at 25 °C for 30 min. The stock solution was then diluted to the syringe concentration of K·mantADP at 4 μM K401 (or K341) plus mantADP at 8 μM. Because K401 is purified with a tightly bound ADP, the labeling procedure would yield a ratio of 2 mantADP plus 1 ADP per K401 active site. The reaction was initiated by rapidly mixing the preformed K·mantADP complex (syringe A) with microtubules stabilized with 10 μM taxol with and without MgATP, MgADP, MgAMP-PNP, or MgATP-γS (syringe B) using a KinTek Stopped Flow System (Model SF-2001, KinTek Corp., State College, PA). All assays were performed at 25 °C in ATPase buffer (20 mM HEPES, pH 7.2 with KOH, 5 mM magnesium acetate, 0.1 mM EDTA, 0.1 mM EGTA, 50 mM potassium acetate, 1 mM DTT) with concentrations reported being the final values after mixing. Fluorescence emission was measured at 450 nm using a 400 nm cutoff long wave pass filter with excitation at 360 nm (Hg arc lamp).

Scheme 1: Alternating Site Mechanism for Dimeric Kinesin

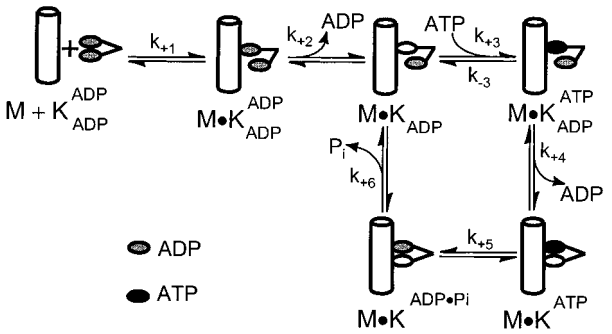

The experiment presented in Figure 3 evaluated the effect on the kinetics of mantADP release using three different isomers of mantATP to generate mantADP. For these experiments K401·ADP was incubated with either 2′mant-3′dATP, or 3′mant-2′dATP, or the mixture 2′(3′)-mantATP at 25 °C for 60 min to hydrolyze the mantATP producing the corresponding mantADP analog. This procedure yielded K401·mantADP complexes that formed via mantATP hydrolysis. The kinetics of mantADP release from these complexes could then be examined.

Data Analysis. The kinetic data from individual experiments were initially fit to either single or double exponential functions. All the kinetic data were then modeled with the KINSIM kinetic simulation program (Barshop et al., 1983) using the single mechanism in Scheme 1 in this paper and Scheme 2 in Moyer et al., (Moyer et al., 1998). Numerical integration with the KINSIM program was used by an iterative process to globally fit the data taking into account the concentrations of K401 (or K341), tubulin, and ATP (or ADP or MgAMP-PNP). The two methods for analysis of kinetic data are discussed in more detail in Moyer et al., (1998). Although the fits obtained by global analysis using computer simulation may not appear as good as those obtained by conventional analysis, one must keep in mind that the number of parameters used to fit the data is considerably larger in the case of conventional fitting. For example, in Figure 2B, only two parameters were adjusted in achieving the best fit to five curves; in contrast, the fitting of those same five curves would require 25 independent parameters to achieve the final fitting (two rates, two amplitudes, and an endpoint, for each curve). Fitting by

[1] Abbreviations: 5′-adenylyl imidodiphosphate (AMP-PNP), adenosine 5′-*O*-(3-thiotriphosphate (ATP-γ-S), Cordycepin 5′-triphosphate (3′-dATP), 2′-deoxyadenosine 5′-triphosphate (2′-dATP), 2′(3′)-*O*-(*N*-methylanthraniloyl)adenosine 5′-diphosphate (mantADP), 2′(3′)-*O*-(*N*-methylanthraniloyl)adenosine 5′-triphosphate (mantATP).

computer simulation provides a more rigorous and precise analysis by fitting the mechanism directly to the data, with no simplifying assumptions. This is especially important with experiments as complex as that presented in Figure 2B.

RESULTS

The experiments presented here measure directly the kinetics of binding of dimeric K401 and monomeric K341 (each containing bound ADP) to microtubules leading to the release of ADP from the microtubule·kinesin·ADP (M·K·ADP) complex. To provide an optical signal for ADP release, we use the fluorescent analog, mantADP, a remarkably good nucleotide analog for kinesin (Gilbert et al., 1995). For the dimeric K401, these experiments resolved the kinetics of the sequential release of mantADP from each motor domain of dimeric kinesin. Microtubule binding stimulates the release of mantADP from kinesin and so the kinetics of mantADP release provide an optical signal to determine the progress of the reaction as one or both kinesin heads bind to the microtubule and release ADP.

Kinetics of mantADP Release from the M·K·mantADP Complex. Figure 1 shows the kinetics of mantADP release after rapidly mixing microtubules with a K401·mantADP complex. The experiment was performed in the presence and absence of added ATP. The results in Figure 1A show that in the absence of added ATP the kinetics of mantADP release are biphasic, suggesting that the motor domains of dimeric K401 bind the microtubule sequentially and with markedly differing rates. The first phase is rapid giving a rate of mantADP release of 163 s^{-1} at 10 μM tubulin. The rate of the fast phase is dependent upon microtubule concentration, and at saturating microtubule concentrations, the rate reaches a maximum of 300 s^{-1} as reported previously (Gilbert et al., 1995). The second phase, accounting for half of the total reaction amplitude, is dramatically slower (2.3 s^{-1} in this experiment). The equal amplitudes of the two phases suggest that the experiment has resolved the kinetics of mantADP release from each motor domain of dimeric K401 after binding to the microtubule. Accordingly, the fast reaction represents the release of mantADP from the first head upon binding to the microtubule and the slow reaction provides a measurement of the rate of release of the mantADP from the second head. It cannot be established unequivocally whether the binding of the second head to the microtubule surface precedes the release of the mantADP. However, the observed rate (2.3 s^{-1}) represents a 200-fold activation of mantADP release from the second head by interaction with the microtubule, whereas the rate of ADP release in the absence of microtubules is less than 0.01 s^{-1} (Gilbert et al., 1995; Sadhu & Taylor, 1992; Ma & Taylor, 1995; Lockhart et al., 1995). This analysis suggests that the second head may interact directly with the microtubule, thereby stimulating mantADP release.

Figure 1A also shows the effect of a high concentration of ATP (1 mM) on the kinetics of mantADP release, leading to an increase in the amplitude of the fast phase with a corresponding reduction in the amplitude of the slow phase. According to our more detailed kinetic analysis described below, these results establish that following the release of mantADP from the first kinesin head, the binding of ATP to the newly vacated nucleotide site stimulates the release of mantADP from the second head. At saturating microtubule concentrations, the rate of release of mantADP from each head reaches a maximum rate of 300 s^{-1}. These results dramatically and directly demonstrate alternating site cooperativity between the two kinesin heads, the central topic of this report.

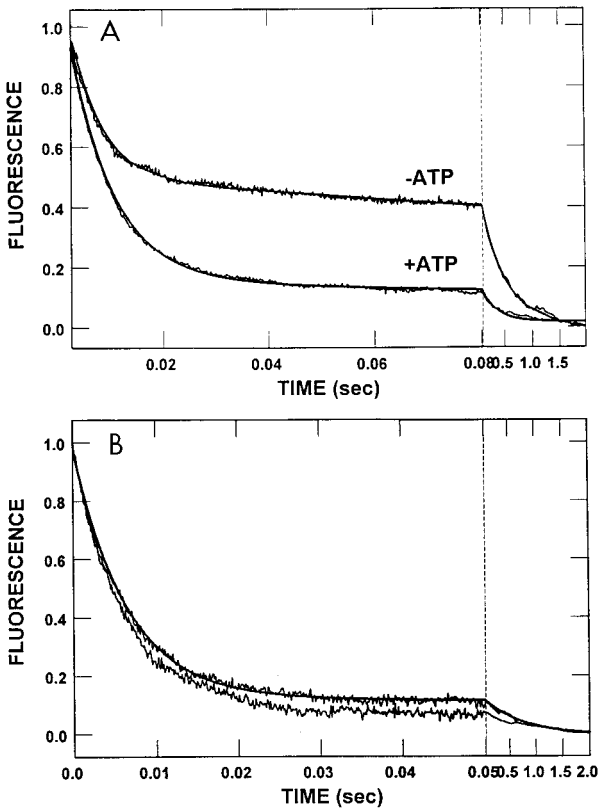

FIGURE 1: Kinetics of mantADP release from the *M*·K·mantADP complex. (A) A representative stopped-flow record of mantADP release in which 2 μM K401·mantADP was rapidly mixed with microtubules (10 μM tubulin) in the presence and absence of 1 mM ATP. The concentrations of K401 and K341 are active site concentrations, and all concentrations reported are final concentrations after mixing. The upper trace shows the experiment in the absence of ATP. The smooth line shows the fit of the data to a double exponential. Note that the kinetics in the absence of ATP are biphasic. The observed rate of the fast phase (first 20 ms) is 163 ± 2 s^{-1} with the relative amplitude $= 0.46 \pm 0.008$. The rate constant for mantADP release at 163 s^{-1} reflects the lower concentration of microtubules used in this experiment. At saturating microtubules, the rate constant for mantADP release is 306 ± 25 s^{-1} as reported previously (Gilbert et al., 1995). The observed rate of the slow phase (0.08−2 s time interval) is 2.3 ± 0.03 s^{-1} (relative amplitude $= 0.48 \pm 0.002$). The lower trace shows the experiment in the presence of ATP. The smooth line is the fit of the data to a double exponential which provided the rate constant of the fast phase $= 122 \pm 0.7$ s^{-1} and the relative amplitude $= 0.75 \pm 0.005$. (B) A representative stopped-flow record of mantADP release in which 2 μM K341·mantADP (monomeric kinesin) was rapidly mixed with microtubules (10 μM tubulin) with and without 1 mM ATP. The traces in the presence and absence of ATP are nearly identical. The fit of the data to a double exponential provided the rate constant for mantADP release at 155 ± 1 s^{-1} (relative amplitude $= 0.84 \pm 0.003$). There is a small residual slow phase (80 ms to 2 s) that is largely independent of ATP. Fluorescence is expressed in arbitrary units, and the curves were normalized to the same maximum increase in fluorescence per active site. For panel A the fluorescence change prior to normalization was 0.9 unit for the sum of the fast and slow phases, and in panel B, the fluorescence change was 0.85 unit prior to normalization.

In order to test whether the observed alternating site kinetics were indeed a function of the dimeric kinesin, the stopped-flow experiments were repeated with K341, a monomeric form of kinesin (Figure 1B) (Correia et al., 1995; Moyer et al., 1996). The time dependence of microtubule-stimulated mantADP release from K341 follows a single exponential at a rate of 155 s^{-1} (at 10 μM tubulin) and reachs a maximum rate of 300 s^{-1} at saturating microtubule concentrations (Moyer et al., 1998). The kinetics are identical in the presence or absence of ATP. In addition, the fluorescence change prior to normalization is 0.85 unit for 2 μM K341 and 0.9 unit for 2 μM K401 active sites, suggesting that the fluorescence change observed represents complete mantADP release from the individual sites of the monomer as well as complete release from both nucleotide sites of the dimer. These results for K341 are expected for a single kinetically independent motor domain. The effect of ATP on the kinetics of mantADP release from dimeric kinesin is due to the binding of ATP to the nucleotide site on one subunit of the dimer.

To define the kinetics of ATP stimulation of mantADP release from dimeric kinesin, we examined the ATP concentration dependence of the reaction in more detail as shown in Figure 2. As the ATP concentration was increased from 0 to 1 mM, the amplitude of the slow phase decreased as the amplitude of the fast phase increased. We interpret this redistribution of fluorescence amplitude to be the result of the slow phase being accelerated by the addition of ATP. Conventional analysis of these reaction kinetics by fitting to a double exponential provides results that appear somewhat confusing at first. With increasing ATP concentration, as the amplitude of the fast phase increases, the rate of the fast phase appears first to decrease and then to increase to a maximum rate. However, this maximum rate is slower than that seen for the fast phase in the absence of ATP because of the two-step sequential mechanism. At high ATP concentration the fast phase represents mantADP from both heads of the dimer. Although the fluorescence signal appears as a single exponential, it represents two fast steps that occur in sequence. Therefore, the observed rate constant for both heads is less than the first head in the absence of ATP. These phenomena can be better understood after quantitative analysis by computer simulation. We used the program KINSIM (Barshop et al., 1983) to fit the data globally to the mechanism shown in Scheme 1 with the rate constants shown in Table 1 to provide the fits to the data shown in Figure 2B. In Figure 2B there is ~2 ms lag predicted by the simulation that corresponds to the steps for K401 binding to the microtubule and ATP binding to the empty site of K401 in the M·K401 complex. This lag is not apparent in Figure 1 because of the 2-ms deadtime of the stopped-flow instrument; however, the curves in Figure 2B are shifted to allow analysis by simulation that starts at time zero after mixing. This comprehensive analysis of the ATP concentration dependence affords estimates for the rates of ATP binding and the rate of ADP release from the second head, as discussed below. Moreover, the quantitative analysis of the rates and amplitudes supports the interpretation that the biphasic kinetics represent the sequential release of mantADP from the two heads of dimeric K401 and that following mantADP release from the first head, ATP binding to the vacant site then stimulates mantADP release from the second head.

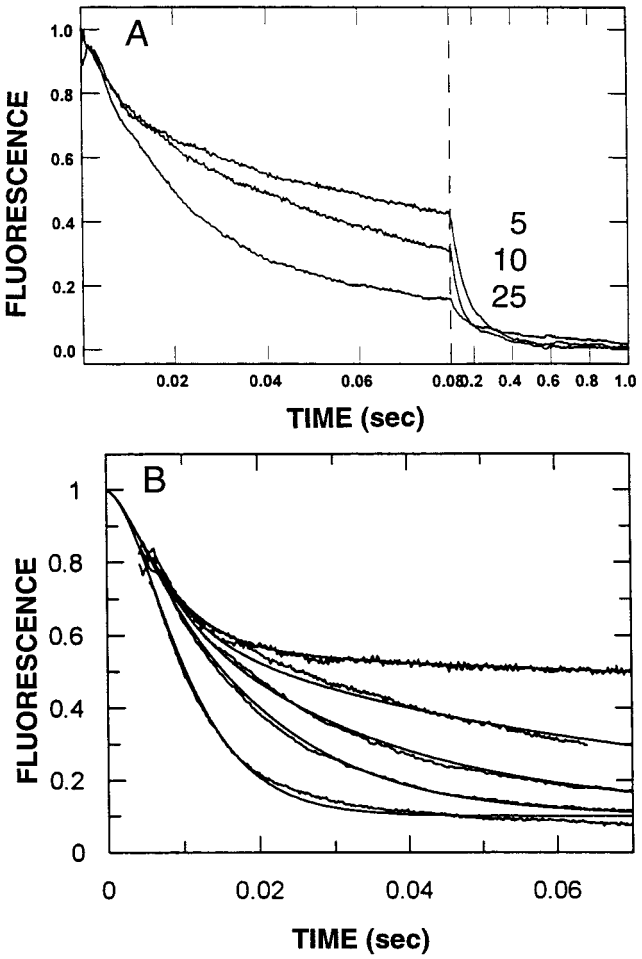

FIGURE 2: ATP concentration dependence of the presteady state kinetics of mantADP release from the M·K·mantADP complex. (A) Representative stopped-flow records of mantADP release in which 2 μM K401·mantADP was rapidly mixed with microtubules (10 μM tubulin) plus ATP at 5, 10, and 25 μM. Note the decrease in the relative amplitude of the slow phase (80 ms to 2 s) as a function of increasing ATP concentration with an increase in the amplitude associated with the fast phase of mantADP release. (B) Representative stopped-flow records of mantADP release in which 2 μM K401·mantADP was rapidly mixed with microtubules (10 μM tubulin) with and without ATP. The transients are shown with the smooth lines representing the global fit of the data to the mechanism in Scheme 1 with $k_{+1} = 20\ \mu M^{-1}\ s^{-1}$, $k_{+2} = 300\ s^{-1}$, $k_{+3} = 2\ \mu M^{-1}\ s^{-1}$, $k_{-3} = 80\ s^{-1}$, $k_{+4} = 300\ s^{-1}$, $k_{+5} = 150\ s^{-1}$, and $k_{+6} = 50\ s^{-1}$. Note that k_{+4} is modeled with rapid rebinding to the microtubule. The ATP concentrations are (from the top trace to the lower trace) 0, 10, 25, 50, and 1000 μM ATP.

Comparison of the Kinetics of mantADP release from the M·K·mantADP Complex Using Three Different Isomers of mantADP. The rate constant for mantADP release at 300 s^{-1} is significantly faster than that reported by Lockhart et al., at 29 s^{-1} for rat K401 (Lockhart et al., 1995) and Ma and Taylor at 38 s^{-1} for human K379 (Ma & Taylor, 1995). We evaluated the possibility that the difference in rate constants reported was dependent upon the mantADP or mantATP used by each group. The routine synthesis of either mantATP or mantADP yields an equilibrium mixture in which the mant fluorophore is attached to either the 2′-hydroxyl (35%) or the 3′-hydroxyl group (65%) (Cremo et al., 1990; Woodward et al., 1991; Moore & Lohman, 1994).

Table 1: Kinetic Constants for the Kinesin ATPase Cycle[a]

	ATP	AMP-PNP
k_{+1}	$19.5 \pm 0.7\ \mu M^{-1}\ s^{-1}$	$19.5 \pm 0.7\ \mu M^{-1}\ s^{-1}$
k_{+2}	$306 \pm 25\ s^{-1}$	$306 \pm 25\ s^{-1}$
k_{+3}	$2 \pm 0.8\ \mu M^{-1}\ s^{-1}$	$0.041 \pm 0.001\ \mu M^{-1}\ s^{-1}$
k_{-3}	$71 \pm 9\ s^{-1}$	
k_{+4}	$300 \pm 100\ s^{-1}$	$30.4 \pm 0.1\ s^{-1}$
k_{+5}	$100 \pm 30\ s^{-1}$	
k_{+6}	$50 \pm 8\ s^{-1}$	

[a] The kinetic constants were obtained as the best global fit to the steady-state and pre-steady-state data by numerical integration using the program KINSIM (Barshop et al., 1983). The rate constants correspond to those in Scheme 1. These rates fit the data presented in this paper in addition to our previously published results (Gilbert & Johnson, 1994; Gilbert et al., 1995). Note that k_{+4} is modeled with rapid rebinding of the motor domain to the microtubule. Steady-state turnover for dimeric K401 is $20 \pm 2\ s^{-1}$ per active site or $40 \pm 4\ s^{-1}$ per dimer, $K_{m,\ ATP} = 61 \pm 8.4\ \mu M$, $K_{0.5,MT} = 0.9 \pm 0.3\ \mu M$.

Although bis-mantADP (mant fluorophore on both the 2′-hydroxyl and 3′-hydroxyl) is also a byproduct of the synthesis, the DEAE Sepharose purification separates bis-mantADP from the monosubstituted nucleotides (Woodward et al., 1991; Moore & Lohman, 1994). Ma and Taylor (1997a; 1997b) reported differences in the mantATP binding kinetics using the different mant nucleotide isomers. We synthesized 2′-mant-3′dATP, 3′-mant-2′dATP, and the mixture of 2′- and 3′-isomers. In our experiments, purified kinesin was incubated with each isomer to permit ADP release from the active site as well as binding of the mantATP derivative and its subsequent hydrolysis. The kinetics of mantADP release from these K401·mantADP complexes were then compared to the kinetics of mantADP release presented in Figures 1 and 2. There was no significant difference in the kinetics of mantADP release using the 2′-mant-3′dATP, 3′-mant-2′dATP, or the mixture of 2′- and 3′-isomers. Furthermore, the mantADP release kinetics were the same for the K401·mantADP complexes obtained either by mantATP hydrolysis (Figure 3) or by mantADP exchange (Figures 1 and 2). The kinetics of mantADP release for the three different isomer preparations of K401·mantADP are comparable as shown in Figure 3. Therefore, we cannot attribute the difference in the rate constant for mantADP release to a difference in the mantADP isomer used in the experiments.

We do not understand the basis for the difference in the mantADP off rate obtained by the different labs. The rate constant measured could reflect in part the source of the recombinant kinesin (*Drosophila* as compared to the mammalian sources, rat and human), and/or the buffer conditions used in the reaction to measure the kinetics, or the subsaturating microtubule concentrations employed. More recently, Ma and Taylor have reported the kinetics of mantADP release from each head of the dimer and from a monomeric kinesin (Ma & Taylor, 1997a; 1997b). They report that at saturating microtubule and ATP concentrations mantADP release from the first head of dimeric kinesin occurs at 50 s^{-1} with mantADP release from the second head at 100 s^{-1}. Therefore, the average rate constant for the two steps in sequence is 33 s^{-1} as reported previously (Ma and Taylor, 1995b). Although we have performed experiments similar to those reported by Ma and Taylor, our rate constants for mantADP release from dimeric K401 and monomeric K341 are significantly faster at 300 s^{-1}.

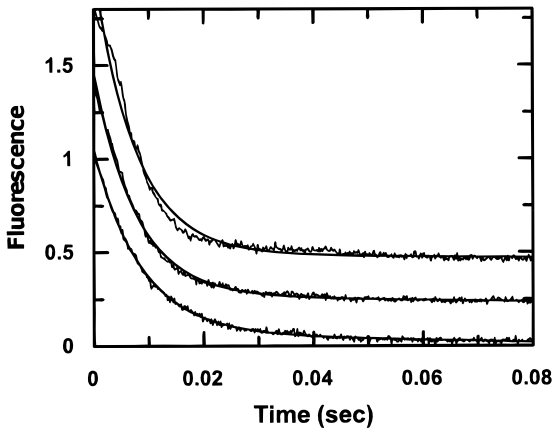

FIGURE 3: Kinetics of mantADP release comparing different isomers of mantADP. Representative stopped-flow records of mantADP release in which the K401·mantADP complex (2 μM) was rapidly mixed with microtubules (10 μM tubulin) plus 1 mM ATP. The K401·mantADP complex was formed by incubation of K401 with 4 μM 2′mant-3′dATP, 3′mant-2′dATP, or the mixture 2′(3′)-mantATP and incubated at 25 °C to form the K401·mantADP complex for each isomer. See Experimental Procedures for specific details. The stopped-flow traces for each isomer have been offset and fit to a single exponential. Note that the traces for each isomer of mantADP are comparable, showing no difference in the pre-steady state kinetics of mantADP release. For 2′-mant-3′dADP (bottom trace) the rate of release is $118 \pm 1\ s^{-1}$ with relative amplitude 0.98 ± 0.004. For 3′-mant-2′dADP (middle trace) the rate of release is $131 \pm 1\ s^{-1}$ with relative amplitude 1.00 ± 0.005. For the mixture of 2′(3′)-mantADP (top trace) the rate of release is $132 \pm 2\ s^{-1}$ with relative amplitude 1.09 ± 0.009. Furthermore, the kinetics of mantADP release from K401·mantADP complexes formed by hydrolysis of mantATP to mantADP at 132 s^{-1} are comparable to the kinetics of mantADP release presented in Figure 1A at 122 s^{-1}. For the Figure 1 experiment, the K401·mantADP complex was formed by exchange of ADP at the active site with 2′(3′)-mantADP.

Effect of Other Nucleotides on mantADP Release. In order to examine in more detail the reactions that stimulate the release of mantADP from the second head, we pursued a series of stopped-flow experiments in which the kinetics of microtubule-induced mantADP release were measured in the presence of nucleotides other than ATP.

Figure 4 shows the effect of ADP on the slow phase of mantADP release after mixing with microtubules. The fast phase of the reaction was unaffected by the addition of ADP. The rate of the slow phase of mantADP release increased as a function of increasing ADP concentration as shown in Figure 4B. The data fit a hyperbola with a maximum rate of 3.8 s^{-1} and an apparent K_d for ADP binding of 152 μM. The rate of mantADP release in the absence of added ADP was 0.4 s^{-1}, implying that the release of mantADP from the second site was activated by microtubules because this rate is at least ~50-fold larger than the rate constant for ADP release in the absence of microtubules.

The rate and amplitude of the slow phase of mantADP release in the absence of nucleotide was somewhat variable. In some experiments, no slow reaction was seen, while the addition of a trace of ADP (1 μM) is sufficient to produce a reproducible amplitude and rate. The observed effect of a low concentration of ADP appears to be due to the need to provide a sufficient amount of unlabeled ADP to provide an effective trap to prevent mantADP from rebinding. However, the effect of higher concentrations of ADP seen

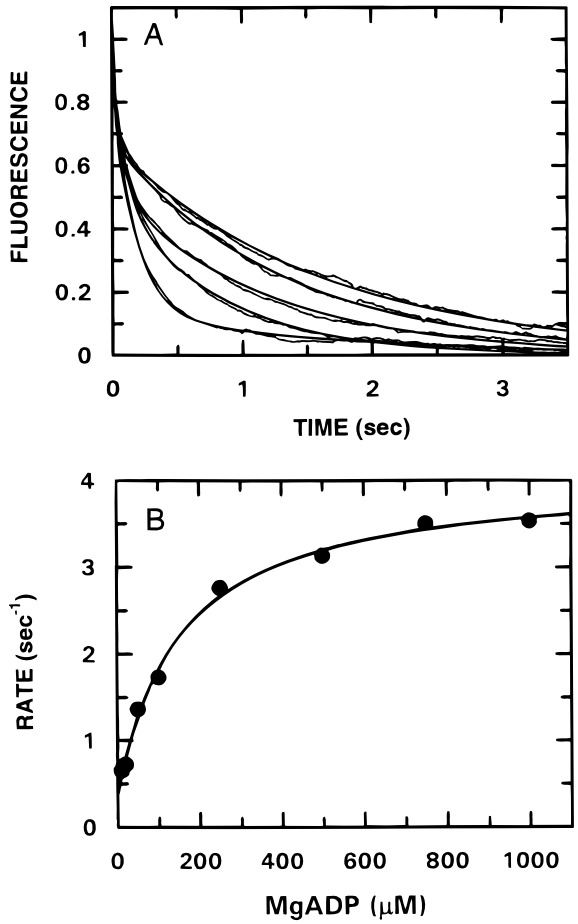

FIGURE 4: Presteady state kinetics of mantADP release from the M·K·mantADP complex as a function of ADP Concentration. (A) 2 μM K401·mantADP was rapidly mixed in the stopped-flow with microtubules (10 μM tubulin) plus ADP (10 μM to 1 mM). Only the slow phase of mantADP release (0.08−5 s, see Figure 1) for each trace is shown in panel A. Upper to lower traces are the experiments at 10, 20, 50, 100, and 500 μM ADP. Each curve was initially fit to a single-exponential function to provide the observed rate constant for release of mantADP from the M·K·mantADP complex shown in panel B. (B) The observed rate constants for mantADP release were plotted as a function of ADP concentration. The fit of the data to the equation $y = k_{max}[ADP]/(K_{d,ADP} + [ADP]) + k_0$ provides the maximum rate constant for mantADP release at saturating ADP concentration, $k_{max} = 3.7 \pm 0.1$ s^{-1}, the rate constant for mantADP release in the absence of nucleotide $k_0 = 0.37 \pm 0.1$ s^{-1}, and the $K_{d,ADP} = 152 \pm 24$ μM. Panel B includes additional data not shown in panel A.

in Figure 4 are clearly due to another phenomenon involving the binding of ADP to a site with an apparent K_d of 152 μM. Accordingly, these data imply that at high concentrations, ADP can bind to the first kinesin head to stimulate the release of mantADP from the second head although the maximum rate is 2 orders of magnitude below the ATP-induced rate.

Requirement of ATP Binding To Induce the Fast ADP Release from the Second Motor Domain. The next question addressed experimentally was whether ATP binding alone was sufficient to induce the rapid release of mantADP from the second head or whether ATP hydrolysis at the first site was required. Figure 5 shows the results obtained with the nonhydrolyzable analog, AMP-PNP. As shown, AMP-PNP stimulates the rate of release of mantADP from the second site to a maximum rate of 30 s^{-1} at saturating AMP-PNP.

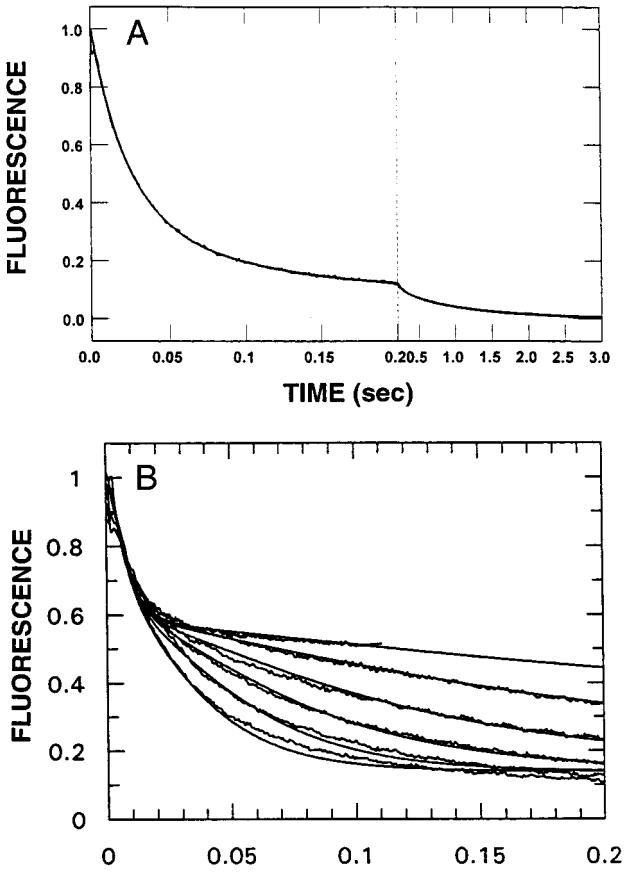

FIGURE 5: Presteady state kinetics of mantADP release from the M·K·mantADP complex as a function of AMP-PNP concentration. (A) A representative stopped-flow record of mantADP release in which 2 μM K401·mantADP was rapidly mixed with microtubules (10 μM tubulin) in the presence of 2.5 mM MgAMP-PNP. (B) AMP-PNP concentration dependence of the presteady state kinetics of mantADP release from the M·K·mantADP complex. Representative stopped-flow records of mantADP release in which 2 μM K401·mantADP was rapidly mixed with microtubules (10 μM tubulin) + MgAMP-PNP. The transients are shown with the smooth lines representing the global fit of the data to the mechanism in Scheme 1 with $k_{+1} = 20$ μM^{-1} s^{-1}, $k_{+2} = 300$ s^{-1}, $k_{+3} = 0.04 \pm 0.003$ μM^{-1} s^{-1}, $k_{+4} = 30$ s^{-1}. The AMP-PNP concentrations are (from the top trace to the lowest trace) 25, 100, 250, 500, 1000, and 2500 μM MgAMP-PNP.

Experiments were also performed with ATP-γS, an ATP analog whose rate of ATP hydrolysis is slowed relative to ATP. The experiments with ATP-γS gave kinetics similar to those observed with AMP-PNP with the slow release of the second mantADP at ~30−40 s^{-1} (data not shown). These results suggest that ATP binding is sufficient, and ATP hydrolysis is not required for the conformational change in kinesin that results in the fast release of mantADP from the second kinesin head.

Although these results are suggestive, they do not establish unequivocally that ATP hydrolysis is not required to achieve the maximal acceleration of mantADP release from the second head. However, we must consider that AMP-PNP and ATP-γS are imperfect analogs of ATP. If binding energy alone, without ATP hydrolysis, were sufficient to induce a change in kinesin structure responsible for the accelerated release of mantATP from the second site, then it is perhaps not surprising that the two analogs provide rates 10-fold slower than that of ATP. Indeed, it is significant that they each accelerate the rate of mantADP release by

approximately 100-fold over the rate seen in the absence of nucleotide. This analysis leads us to the tentative conclusion that in the reaction pathway with ATP ATP binding is sufficient to stimulate the release of ADP from the adjacent site. Thus, the interactions that result from ATP binding at the first site provide the energy to induce a change in protein structure leading to rapid mantADP release from the second motor domain.

DISCUSSION

The results presented have provided direct evidence for alternating site cooperativity between the catalytic domains of the kinesin dimer in that ATP binding to the first site stimulates release of ADP from the second site. These experiments also indicate that the active sites of dimeric kinesin differ in their nucleotide binding states (ATP, ADP·P_i, or ADP) under conditions of processive movement. At any one time, the two heads are at different steps of the ATPase cycle. Scheme 1 presents the minimal mechanism and kinetic constants, summarized in Table 1, based on the results presented in this paper and the companion paper (Moyer et al., 1998) as well as those published previously (Gilbert & Johnson, 1994; Gilbert et al., 1995).

Experimentally, we enter the ATPase cycle by adding a dimeric kinesin molecule containing ADP bound to both sites. The first motor domain binds to the microtubule leading to the rapid release of ADP from the active site; this reaction will not be part of the normal ATPase cycle, except as the first step of reaction when kinesin rebinds to the microtubule after completely dissociating into solution. After the release of ADP from the first head, ATP binds to the newly vacated active site stimulating the second head to bind to the microtubule and release its ADP at a fast rate. In order to complete a cycle of processive ATP turnover, we postulate that ATP hydrolysis then occurs at the active site of the first head followed by the rate-limiting step of the pathway involving release of phosphate and release of the motor domain from the microtubule, which is coupled to the tight binding of the other head to the microtubule. The cycle is then repeated for the second head. One turnover of ATP on a given head requires two turns around the cycle. In order to better understand the cycles in Scheme 1, one has to invert the images of the two heads at step 6 involving phosphate release to complete two turns around the cycle with each head.

Our experimental evidence to date cannot distinguish if phosphate release occurs while the motor domain is still bound to the microtubule or if phosphate release occurs after detachment from the microtubule. We only know that the two processes, phosphate release and release of kinesin from the microtubule, are coupled kinetically. The equilibrium binding studies of Rosenfeld et al., (1996) with another dimeric kinesin construct show that inorganic phosphate reduces the affinity of dimeric kinesin for microtubules, consistent with a model in which phosphate release follows the detachment of K·ADP·P_i from the microtubule.

The data presented here with our previously published results (Gilbert et al., 1995) establish that the rate-limiting step occurs after ATP hydrolysis and leads to the release of the K·ADP motor domain from the microtubule. Steady state turnover for dimeric K401 is 20 s^{-1} per site or at 40 s^{-1} per dimer. Because of the alternating site cooperativity, the intrinsic rate constant for the rate-limiting step of the pathway reflects steady state turnover for dimeric kinesin rather than the per site rate constant at 20 s^{-1}. Accordingly, the intrinsic rate constant for the release of the first head of dimeric kinesin from the microtubule is at least 50 s^{-1} rather than the 20 s^{-1} assigned previously (Gilbert et al., 1995).

An important conclusion of these studies is that ADP release is a fast step. Measurement of the microtubule concentration dependence afforded extrapolation to a value of approximately 300 s^{-1} for the maximum rate of the two-step ADP release in the presence of 1 mM ATP (Gilbert et al., 1995). An observed rate of 300 s^{-1} would require rates of approximately 600 s^{-1} for each of the individual ADP release steps in the two-step sequence. However, analysis by computer simulation of the time course of the reaction at subsaturating microtubule concentration has shown that the data can be adequately fit by rates of approximately 300 s^{-1} for each step, and so we have placed less emphasis on the rates obtained by extrapolation. Regardless of the magnitude of the ADP release rate, it is far to fast to contribute significantly to the net rate of steady state ATP turnover.

We were somewhat surprised to see a rate of 0.4 s^{-1} for mantADP release in the absence of ATP (Figure 4) because this rate was significantly faster than ADP release in the absence of microtubules at 0.01 s^{-1}, suggesting that the second motor domain binds the microtubule in the absence of added nucleotide. Previous experiments of Hackney (Hackney, 1994) reported the release of the second ADP to be exceedingly slow in the absence of ATP, resulting in a tethered dimer in which one motor domain was bound tightly to the microtubule while the other motor domain was not bound to the microtubule and still retained its ADP. Ma and Taylor (1997b) have also reported a long lifetime species, in the absence of added nucleotide, with one kinesin head bound to the microtubule and with the other detached from the microtubule but bound to ADP, but there is some confusion as to the lifetime of this species. Some of the experiments reported by Ma and Taylor (1997b) describe a stable species present in equilibrium while other experiments define a rate of 0.5 s^{-1} for the release of the second ADP molecule. While we also present evidence for the existence of this species, we have shown that its lifetime is short under our conditions, exhibiting a release rate of 0.4−2 s^{-1}.

The variability in the lifetime of the kinesin isomer with one head detached from the microtubule is also mirrored in the observations by electron microscopy. Hirose et al., (Hirose et al., 1996) presented three-dimensional cryoelectron microscopy images of dimeric kinesin in the presence of AMP-PNP in which one motor domain appeared to be bound to the microtubule while the other was unattached. However, our analysis by electron microscopy (Harrison et al., 1993) revealed a decoration of kinesin with an 8 nm repeat and a stoichiometry of one kinesin monomer per tubulin, implying that both heads were bound to the microtubule under our conditions. We interpret these differences to reflect how conditions in different laboratories reveal different states of the force production cycle. At one point in the cycle, one head of kinesin is detached while at a later step in the cycle both heads are attached, and it is understandable that different solution conditions could favor one state or the other. Moreover, the observations *in vitro* in the absence of ATP

are rather artificial and differences in the lifetimes of the one-head-detached state may not be significant in terms of the pathway of ATP turnover *in vivo*. The important observation is that the binding of ATP greatly stimulates the release of ADP from the second head and this reaction is coupled to the interaction of that head with the microtubule.

Although in solution the two heads are identical, upon interaction with the microtubule they become different. This asymmetry is essential to the alternating site mechanism of force production. Although the mechanism of force production cannot yet be ascertained, the results presented here provide a basis for a plausible model for the nature of the rate-limiting step in force production. In our previous analysis, we proposed that the rate-limiting step in a single ATP turnover is the release of the kinesin·ADP·P_i complex from the microtubule following hydrolysis at the active site (Gilbert et al., 1995). Although it is most reasonable to postulate that force production occurs at the slowest step of the pathway, force production cannot occur in a reaction leading to weaker binding of the kinesin to the microtubule. The present results resolve this controversy by suggesting that the rate-limiting release of one kinesin head from the microtubule be coupled to the tighter binding of the other kinesin head to the microtubule. Thus, force production is a function of the coordinated activities of the two kinesin heads, with the reactions leading to tight binding of one kinesin head governed by the rate-limiting release of the adjacent kinesin head from the microtubule after ATP hydrolysis. Thus, we can no longer think of force production cycles in terms of the reactions occurring on single ATPase sites. Moreover, the alternating site mechanism employed by kinesin affords an efficient method for processive movement in which at least one head remains tethered to the microtubule throughout the cycle. Analysis of the kinetics of ATP turnover by single-headed kinesin, described in the accompanying paper, reveals further information on the nature of the interactions between the subunits of the dimer (Moyer et al., 1998).

In summary, the results presented have provided new information about the interactions of the motor domains of dimeric kinesin with the microtubule. These studies have provided direct evidence for alternating site cooperativity of the kinesin motor domains in which ATP binding at one catalytic site stimulates the rapid release of ADP from the second kinesin motor domain. Furthermore, it is the coordination of the ATPase cycles of dimeric kinesin that establishes the processivity for interactions with the microtubule.

ACKNOWLEDGMENT

We thank Dr. Smita Patel (Ohio State University, Columbus, OH) and Dr. Michael Geeves (Max-Planck-Institut für Molekulare Physiologie, Dortmund, Germany) for critically reviewing earlier versions of the manuscript and N. R. Lomax of the National Cancer Institute for taxol.

REFERENCES

Barshop, B. A., Wrenn, R. F., & Frieden, C. (1983) *Analytical. Biochem. 130*, 134.

Berliner, E., Young, E. C., Anderson, K., Mahtani, H. K., & Gelles, J. (1995) *Nature (London) 373*, 718.

Block, S. M., Goldstein, L. S. B., & Schnapp, B. J. (1990) *Nature (London) 348*, 348.

Correia, J. J., Gilbert, S. P., Moyer, M. L., & Johnson, K. A. (1995) *Biochemistry 34*, 4898.

Cremo, C. R., Neuron, J. M., & Yount, R. G. (1990) *Biochemistry 29*, 3309.

Gilbert, S. P., & Johnson, K. A. (1993) *Biochemistry 32*, 4677.

Gilbert, S. P., & Johnson, K. A. (1994) *Biochemistry 33*, 1951.

Gilbert, S. P., Webb, M. R., Brune, M., & Johnson, K. A. (1995) *Nature (London) 373*, 671.

Hackney, D. D. (1994) *Proc. Natl. Acad. Sci. U.S.A. 91*, 6865.

Hackney, D. D. (1995) *Nature (London) 377*, 448.

Harrison, B. C., Marchese-Ragona, S. P., Gilbert, S. P., Cheng, N., & Steven, A. C. J. (1993) *Nature (London) 362*, 73.

Higuchi, H., Muto, E., Inoue, Y., & Yanagida, T. (1997) *Proc. Natl. Acad. Sci. U.S.A. 94*, 4395.

Hiratsuka, T. (1983) *Biochim. Biophys. Acta 742*, 496.

Hirose, K., Lockhart, A., Cross, R. A., & Amos, L. A. (1995) *Nature (London) 376*, 277.

Hirose, K., Lockhart, A., Cross, R. A., & Amos, L. A. (1996) *Proc. Natl. Acad. Sci. U.S.A. 93*, 9539.

Howard, J., Hudspeth, A. J., & Vale, R. D. (1989) *Nature (London) 342*, 154.

Hua, W., Young, E. C., Fleming, M. L., & Gelles, J. (1997) *Nature (London) 388*, 390.

Huang, T. G., Suhan, J., & Hackney, D. D. (1994) *J. Biol. Chem. 269*, 16502.

Hunt, A. J., Gittes, F., & Howard, J. (1994) *Biophys. J. 67*, 766.

Inoue, Y., Toyoshima, Y. Y., Iwane, A. H., Morimoto, S., Higuchi, H., & Yanagida, T. (1997) *Proc. Natl. Acad. Sci. U.S.A. 94*, 7275.

Jiang, W., & Hackney, D. D. (1997) *J. Biol. Chem. 272*, 5616.

Kull, F. J., Sablin, E. P., Lau, R., Fletterick, R. J., & Vale, R. D. (1996) *Nature (London) 380*, 550.

Lockhart, A., Crevel, I. M.-T. C., & Cross, R. A. (1995) *J. Mol. Biol. 249*, 763.

Lockhart, A., Cross, R. A., & McKillop, D. F. A. (1995) *FEBS Lett. 368*, 531.

Ma, Y.-Z., & Taylor, E. W. (1995a) *Biochemistry 34*, 13233.

Ma, Y.-Z., & Taylor, E. W. (1995b) *Biochemistry 34*, 13242.

Ma, Y.-Z., & Taylor, E. W. (1997a) *J. Biol. Chem. 272*, 717.

Ma, Y. Z., & Taylor, E. W. (1997b) *J. Biol. Chem. 272*, 724.

Meyhöfer, E., & Howard, J. (1995) *Proc. Natl. Acad. Sci. U.S.A. 92*, 574.

Moore, K. J. M., & Lohman, T. M. (1994) *Biochemistry 33*, 14550.

Moyer, M. L., Gilbert, S. P., & Johnson, K. A. (1996) *Biochemistry 35*, 6321.

Moyer, M. L., Gilbert, S. P., & Johnson, K. A. (1998) *Biochemistry 37*, 800−813.

Ray, S., Meyhofer, E., Milligan, R. A., & Howard, J. (1993) *J. Cell Biol. 121*, 1083.

Romberg, L., & Vale, R. D. (1993) *Nature (London) 361*, 168.

Rosenfeld, S. S., Rener, B., Correia, J. J., Mayo, M. S., & Cheung, H. C. (1996) *J. Biol. Chem. 271*, 9473.

Sadhu, A., & Taylor, E. W. (1992) *J. Biol. Chem. 267*, 11352.

Schnitzer, M. J., & Block, S. M. (1997) *Nature (London) 388*, 386.

Song, Y. H., & Mandelkow, E. (1993) *Proc. Natl. Acad. Sci. U.S.A. 90*, 1671.

Svoboda, K., Mitra, P. P., & Block, S. M. (1994) *Proc. Natl. Acad. Sci. U.S.A. 91*, 11782.

Walker, R. A. (1995) *Proc. Natl. Acad. Sci. U.S.A. 92*, 5960.

Woodward, S. K. A., Eccleston, J. F., & Geeves, M. A. (1991) *Biochemistry 30*, 422.

BI971117B